Turbulence Characteristics in Particle Laden Water Jet Injected Into Water Tank by Means of PDA and PIV

by

Ismail M. Youssef, Tsuneaki Ishima, Takashi Shimokawara and Tomio Obokata.

Dept. of Mechanical System Engineering

Gunma University

1-5-1, Tenjin, Kiryu, 376-8515 JAPAN

ABSTRACT

Measurement on particle motion and analysis on turbulence modification at the liquid-solid two-phase jet flows were carried out in the paper. The water jet including glass beads of 375 μm in mean diameter was injected into still water bath. To study the particle dispersion near the region of jet outlet, the initial velocity gradient was changed with injection pipe conditions, which had 5 and 8 mm in diameter, with injecting velocities of 1.8 and 1.5m/s, respectively. Firstly, an LDA was applied to measure the particle velocity. The Saffman's lift force and Stokes number based on the time constant of the particle and inverse of the velocity gradient of water were estimated from the experimental results. Figure 1 shows the relationship between the Stokes number and relative velocities between particle and water. Figure 2 shows the Saffman's lift force. Detail discussion about them is presented in this paper. Secondly, particle mass loading was changed to discuss the turbulent modification. The PDA raw data were divided into particle and water velocities. Figure 3 illustrates the variation in turbulent intensity against local mass loadings. The positive correlation can be clearly found in the figure. Finally, a particle image velocimetry (PIV) was used to implement the two-phase flow measurement. To analyse the present flow, two-types of light sources, YAG laser and stroboscope light, were employed. Stroboscope light can only be used for big and small velocity particles' motion because of its poor light intensity. In the contrary, seeding particles data could be obtained by using the YAG double pulse laser. Comparing between PIV and PDA data, it seems that the PIV data with the YAG double pulse laser is close to seeding particle velocities measured by PDA. It is pointed out that the PIV can measure with discrimination of large particles and small seeding particles by changing the light source power.

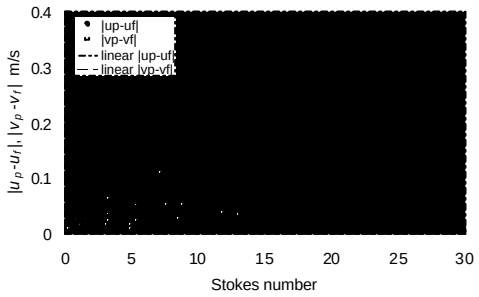

Fig. 1 Relative velocities between particle and water versus Stokes number.

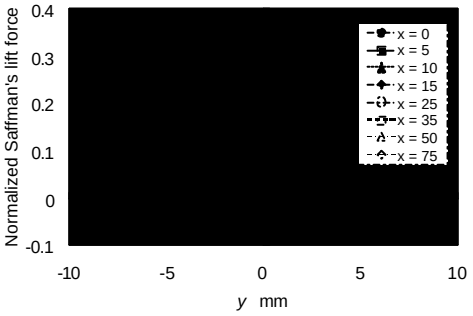

Fig. 2 Distribution of Saffman's lift force.

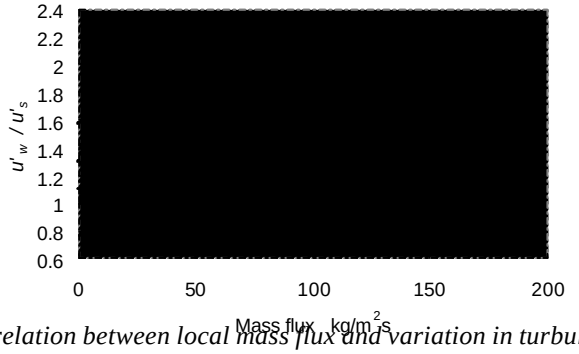

Fig. 3 Correlation between local mass flux and variation in turbulence intensity.

1. INTRODUCTION

The particle dispersion and turbulence modification are of interest in many industrial processes, for example, combustion system, spray flow, pulverized coal combustion and so on. Many researchers have been studying about these subjects (for example, Taylor (1921), Snyder and Lumley (1971), Wells and Stock (1983), Chein and Chung (1987), Hishida et al. (1992), Ishima et al. (1993)). Especially, the two-phase jet flow is one of the fundamental flow structures. The single phase jet flow is well known about its features. A comparison between the results of single phase and two-phase flows can indicate and discuss the turbulence modification caused by particle and the particle dispersion in the jet flow. In the two-phase flow, the important factor is an interaction between particle and turbulent motion of the fluid. In the experiments of solid-water two-phase flow, this interaction becomes more important because the density ratio between both phases is smaller compared with that of gas-solid two-phase flow. And larger Reynolds number can be easily realized in the water flow. Therefore, the present study will focuse on clarifying the solid-water two-phase jet flow. The solid-water two-phase flow experiments were carried out by Calabrese and Middleman (1976), Parthasarathy and Feath (1987), Hishida et al. (1989) and the authors (1994). In the paper of the Calabrese and Middleman, the particle had a diameter of which range is almost the same as turbulent scale. The particle motion was measured by using visualization techniques. Parthasarathy and Feath and the authors studied about the particle motion and Hishida et al. showed the turbulent modification. About the particle dispersion, the published data indicated the importance of the phenomena near region of jet exit. The importance of the jet exit was also pointed out by several researchers of Snyder and Lumley (1971) and Hardalupas et al. (1989). However, detail information has not been reported. In the present study, comprehensive measurements of the two-phase flow are planed for understanding the particle motion at the nozzle exit and around it.

On the other hand, the turbulent modification was discussed by a famous paper described by Gore and Crowe (1989). They indicated that the ratio of particle diameter to turbulence length scale is the dominant factor for turbulent modification in two-phase flow. However, there seems to be still unknown factors, for instance, particle loading and density. In a dilute condition of particle concentration, the turbulence cannot be influenced by the particle concentration and particle motion is dependent on the turbulence motion (one-way coupling). When the particle concentration becomes densely, the turbulence modification cannot be negligible. This simple phenomenon means the particle loading is also important parameter in the two-phase flow. In this study, the relationship between particle mass flux and variation in the turbulence will be discussed. All of above experiments were planned with using laser techniques, namely a laser Doppler anemometer (LDA) and a phase Doppler anemometer (PDA). Especially, the PDA can provide the particle velocity and diameter, then it is possible to measure the velocities of fluid phase and particle simultaneously. The size discrimination can be applied using the results of diameter data measured by PDA. It is expected to discuss detail turbulent modifications.

Recently the particle image velocimetry (PIV) can provide useful data for understanding the flow structures. In the study, PIV was also applied to measure the two-phase jet. Some tests were tried for understanding the characteristics of the PIV data.

2. EXPERIMENTAL APPARATUS

2.1 Flow Condition and Configuration

Figure 4 shows the experimental setup. The test section was set vertically where the particle lateral motion was independent from the gravity. The water jet was injected from pipes of 5 and 8mm in diameter, respectively. The mean velocity on the axis of the water jet was set to 1.8 and 1.5 m/s for 5 and 8 mm pipe, respectively. The Reynolds numbers which based on the mean velocity and pipe diameters were 7.8×10^3 and 1.04×10^4 for 5 and 8mm diameter pipes respectively. Since the flow rate from the injection pipe is too small compared with the total capacity of test section, surrounding recirculation flow formed by the water jet can be neglected. The glass beads of 375μm in mean diameter were released in the upstream of the jet and they were mixed well in the particle injector, then injected as the particle laden water jet into the test section that is filled with still water. To study the effect of local mass loading on the turbulent characteristics, two conditions of particle concentration were chosen, that is, dilute-condition with the initial mass loading to 0.087% and dense-condition with the initial mass loading as 0.305%. The origin of coordinate was set on the center of the jet pipe and *x*- and *y*-axes were set to the flow direction and the horizontal direction, respectively. Figure 5 illustrates an example of the measuring positions of LDA.

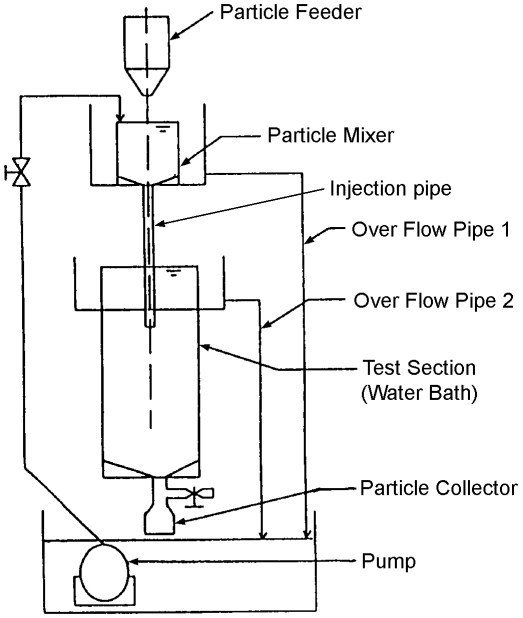

Fig.4 Experimental apparatus.

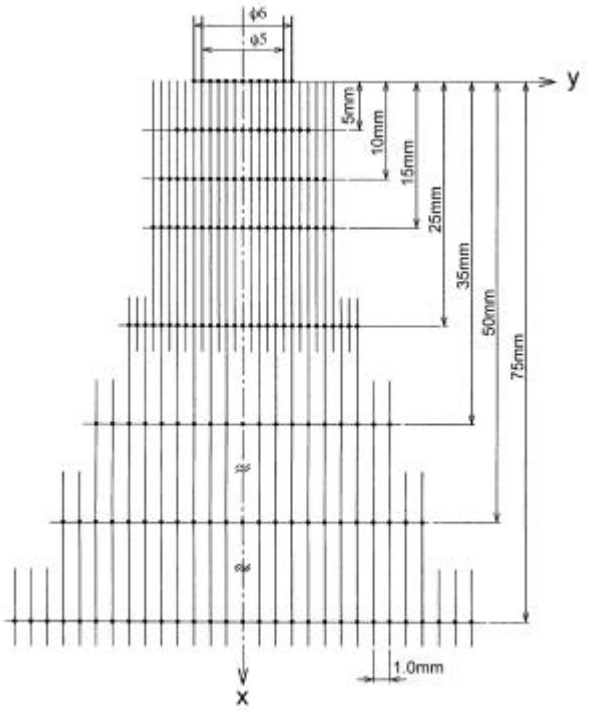

Fig. 5 Measurement points.

2.2 Experimental Techniques

A laser Doppler anemometer (LDA) was applied for measuring both of the particle velocity and water velocity independensly under the condition of dilute two-phase flow. The sending optics of the LDA consisted of He-Ne laser source with 10 mW power, double bragg cell as 80 and 83 MHz and transmitting lens of 300mm focal length, then the half angle of beam intersection is equal to 3.81 degree. Seeding particle of Al_2O_3, with mean diameter of about 2 μm, was used for water velocity measurement. A counter type signal processor (DISA 55L90a) processed the Doppler signal and statistic values of mean velocity and fluctuation velocity were calculated by a PC. During the measurement of the water velocity in two-phase flow, a threshold window was used for discriminating the signal from seeding particles. Under the dense condition, for the purpose of simultaneous velocity measurement of both phases, a phase Doppler anemometer (PDA) system (Aerometrics PDPA) was applied. Measurement parameters were set as the followings: focal length of transmitting lens 495 mm, receiving angle 30 degree, the half angle of beam intersection 0.73 degree and diameter range 5.2 to 769 μm. The raw data mode was selected and the data were divided into seeding and glass particles velocities by particle diameters. According to the diameter range limitation of PDPA, in which maximum diameter is set to 30 times larger than the minimum diameter, particles under 20μm were treated as seeding particle and particles between 350-400μm were treated as glass particles. This slightly large upper limitation of seeding seems to be not enough to follow the water flow, but the particle relaxation time, defined as $(2\rho_p + \rho_f)d_p^2/36\mu$ where ρ is the density of the particle and water and μ is the fluid viscosity, is about 60μs. Then, the relaxation time is small enough to follow the fluid motion. The local mass loadings were calculated from the mean data rate, which was calculated by dividing the attempt number count of the Doppler signal by measuring run time, mean velocity and probe area which was assumed to be fixed value. The local mass loading was obtained not only from the data of LDA but also PDA.

Recently, Particle Image Velocimetries (PIV) are applied to measure the two dimensional velocity map in the measuring plane at an instantaneous time. Generaly speaking, the PIV can provide more useful data, but they don't include diameter information. In this paper, the potential of the PIV measurements are also discussed. The PIV data processor used in this study is Flow Map PIV 2000 made by Dantec. For the PIV measurements, two light-sources, YAG laser and stroboscope, were tested. Then, the data were compared with that of PDA. It is difficult to use the stroboscope to get a good picture because of poor light intensity. The velocity of initial jet was set as from 0.057 to 0.7 m/s. These small velocities are only acceptable by the stroboscope light to get flow pictures. The interrogation areas were set as 64 pixels square and 128 pixels square. Total measuring areas were 37.6 x 38.0 mm for measurement with YAG laser and 35.4x35.8 mm with stroboscope.

3. RESULTS AND DISCUSSIONS

3.1 Results under Dilute Concentration

Figures 6(a)-(c) show the distributions of streamwise mean velocities of single-, water- and particle phases at x = 0, 10 and 75 mm for D = 5mm, respectively. All of the velocities were normalized by using the center line velocity of the single phase flow U_m, and y positions were normalized by half width b. The velocities of single phase and water phase (in two-phase flow) have very similar distributions at all of the measurement lines. In figure 6(a) with x = 0 mm, a dashed line indicates the pipe flow distribution with Reynolds number of 4.0×10^3 introduced by Schlichting (1955). It is clear that the all of the velocities are on the dashed line and the jet has the velocity profiles of the fully developed pipe flow distribution. Then, in Fig. 6(b) with x = 10 mm, the distribution quickly becomes similar to the gaussian distribution indicated as solid line. The water phase can follow this change in the mean velocity, however particle cannot, and then particle has relative velocity at the outer sides of the jet, $|y/b| > 1$. On the other hand, around the center line, the relative velocity is small because that the mean velocity maintains the value at the jet outlet on the center line during the certain distance from the outlet. This region is almost the same situation as "potential core" of the jet flow. At x = 75 mm shown in Fig.6 (c), the distributions of single and water phases are close to the gaussian distribution. The particle has the relative velocity at all of the positions. The relative velocities are almost same value in each position and the value is equal to the terminal velocity of the particle, 0.061m/s. Figures 6 (d) and (e) shows the results under the condition of D = 8 mm, while x = 0 and 75 mm, respectively. The tendencies of mean streamwise velocities are close to that of D = 5 mm.

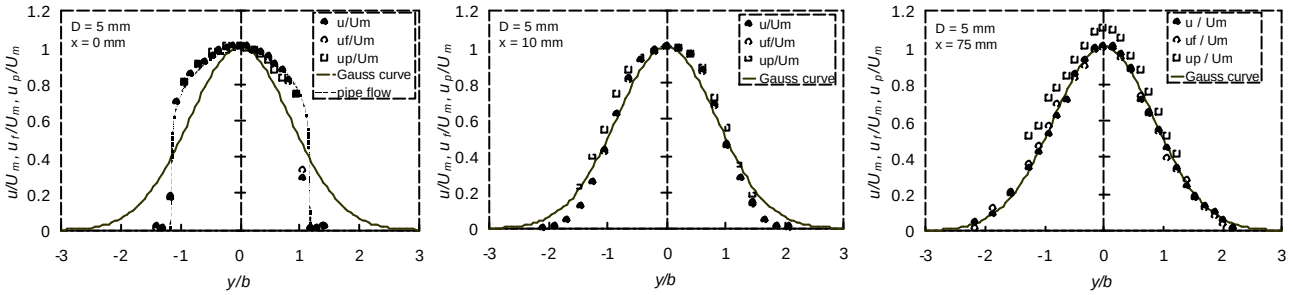

(a) D = 5 mm, x = 0mm. *(b) D = 5 mm, x = 10mm.* *(c) D = 5mm, x = 75mm.*

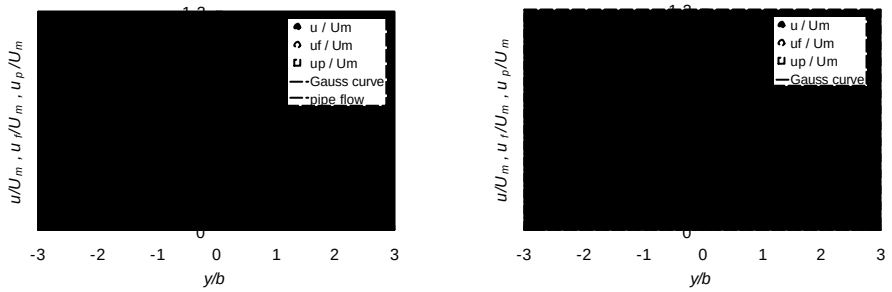

(d) D = 8 mm, x = 0mm. *(d) D = 8 mm, x = 75mm.*

Fig.6 Radial profiles of mean axial velocities for D = 5 and 8 mm.

Figures 7 (a) and (b) shows the streamwise fluctuation velocities of single phase, water and particle phases in two-phase flow at x = 0 and 75 mm with D = 5 mm, respectively. The fluctuation velocities were normalized by jet outlet mean velocity (Ui). The particle fluctuation at the x = 0 mm exceeds those of single phase and water phase. In the downstream, all of the fluctuations become close to each other. The fluctuation of water phase is the same as that of single phase flow because of the dilute condition. Figures 7 (c) and (d) shows the results with D = 8 mm. The overall tendencies are the same as that of D = 5 mm. At x = 0 mm, the particle fluctuation also exceed those of single and water phases but the value is close to the single and water phases. Under the condition of D = 8 mm the velocity gradient is smaller than that of D = 5mm. It is considered that the velocity gradient plays important role on the particle motion.

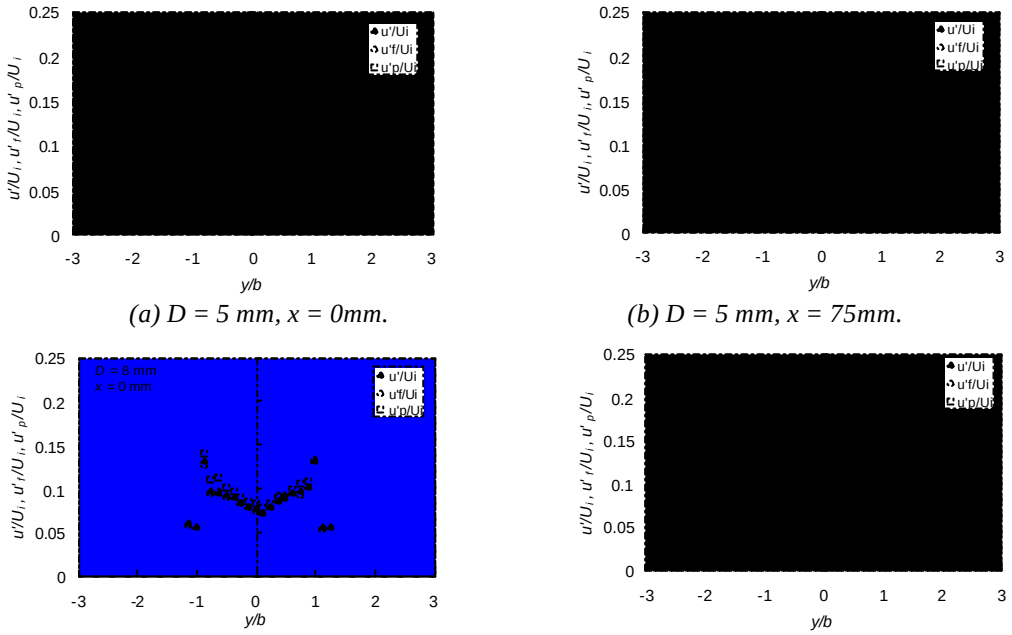

(a) D = 5 mm, x = 0mm. *(b) D = 5 mm, x = 75mm.*

(c) D = 8 mm, x = 0mm. *(d) D = 8 mm, x = 75mm.*

Fig.7 Radial profiles of axial fluctuation velocities for D = 5 and 8 mm.

Figure 8 illustrates the streamwise relative velocity between water phase and particle. The relative velocity on the jet outlet is almost equal to zero. At x = 5 mm, the relative velocity is suddenly increase. In the downstream of x = 5 mm, the relative velocities are gradually decrease. Figures 9 (a) and (b) shows the lateral relative velocities for D = 5 and 8 mm, respectively. Comparison between Figs. 9(a) and 9(b), the result with D = 5 mm is lager than that of D = 8 mm. The change in the pipe diameter means variation of the velocity gradient. The velocity gradient under the condition of D = 8 mm is smaller than that of D = 5 mm. The lateral relative velocities seem to be influenced by the velocity gradient.

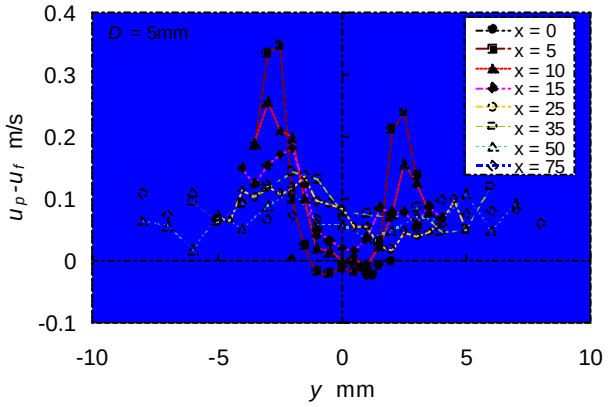

Fig. 8 Relative velocity between particle and water in streamwise direction with D = 5mm.

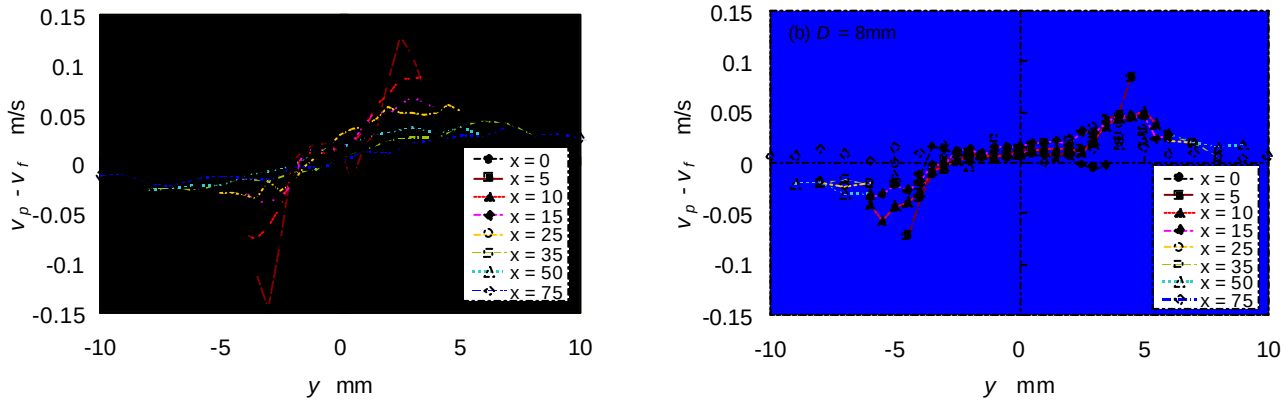

(a) D = 5mm. *(b) D = 8mm.*

Fig. 9 Relative velocity between particle and water in lateral direction with two pipe diameters.

It is considered from Figs. 6-9 that the particle motion is dependent on the velocity gradient. Then, time scales and Stokes number are estimated as followings;

$$St = t_p / t_f, \quad where \quad t_p = \frac{(2r_p + r_f) \cdot d_p^2}{36m}, \quad t_f = \frac{1}{du_f / dy}$$

where t_p and t_f are particle and water time constants, r_p and r_f are densities of glass particle and water, d_p is mean diameter of glass particle, m is water viscosity and u_f is mean velocity of water (in two-phase flow).
The Stokes number obtained here means the ability of the particle tracing to the water mean motion. The relationship between Stokes number and relative velocity in both directions is shown in Fig. 10. The positive correlation can be seen in this figure. The streamwise relative velocity is larger than the lateral relative velocity. In the streamwise direction, the relative velocity around Stokes number equals to zero is scattered. In this figure, all of the data are included and no terminal velocity effect is considered. Since the particle has relative velocity caused by terminal velocity in the downstream where the Stokes number is small, this may be the reason for the result shown in Fig. 10 is scattered. The linear approximation line of stramwize relative velocity is larger than that of lateral direction because the lateral motion of the particle is hardly affected by the streamwise motion. The Stokes number is obtained by using the streamwise mean velocity, then the correlation between the Stokes number and lateral relative velocity becomes small. Note that the Stokes number is obtained by streamwise direction but the lateral relative velocity has positive correlation. This phenomenon indicates that the lateral particle motion is affected by both of lateral and streamwise mean water velocity.

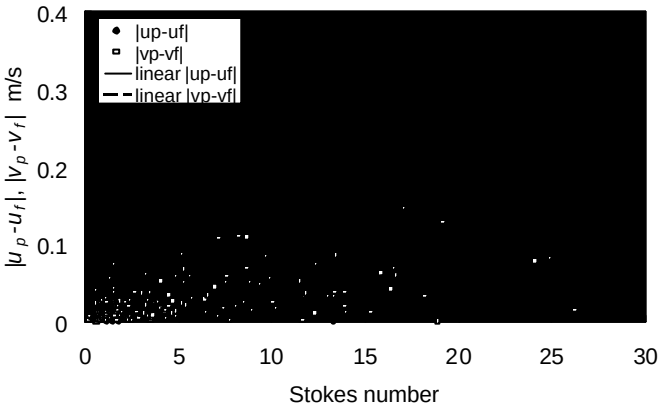

Fig. 10 Relationship between Stokes number and relative velocities of both direction.

The Saffman's lift force was calculated by

$$F_{saff} = .1.61 d_p \cdot |u_f - u_p| \sqrt{\mathrm{Re}_G}, \quad \mathrm{Re}_G = \frac{d_p^2}{n} \cdot \frac{du_f}{dy}$$

Figure 11 shows the results of the Saffman's lift force. The results of Saffman's lift force were normalized by using gravity acting on one particle with mean diameter of 385 μm. The maximum force acts at the x = 5 mm, and in the downstream the force is gradually decreasing. It is considered from figures 10 and 11 that the particle cannot follow the mean water motion due to their large Stokes number and then it has a large relative velocity on the jet outlet and near region of the pipe exit. The large relative velocity causes the large Saffman's lift force. Then, particle can disperse lateral direction quickly near region of pipe exit. Change in the pipe diameter, for controlling the velocity gradient, affects the particle motion and dispersion due to different Stokes number and Saffman's lift force.

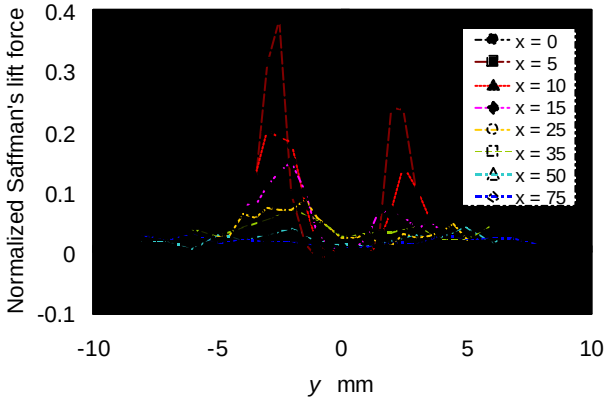

Fig. 11 Normalized Saffman's lift force.

3.2 Results under Dense Concentration

Figure 12 (a) and (b)shows the mean velocities with the dense condition for x = 0 and 50 mm, respectively. The particle mean velocity at x = 0 mm is larger than the water phase. The velocity distribution of water phase is different from the single-phase flow. These features cannot be observed in the dilute condition shown in Fig. 6. In the dense condition, the gravity plays dominant role on the particle motion. The water phase is affected by the particle motion. Comparison of distributions of single phase and water phase indicates that the distribution shape of single phase flow is close to the parabolic curve on the contrary that of water phase is near top-hat type shape. There are two possibilities of the reason why the distribution become close to the top-hat shape. The first one is that particles act as like the turbulent promoter. The particles make turbulent fluctuation and transition from laminar to turbulence is occurred in the pipe flow. The second one is that development of the pipe flow is disturbed, then the shape becomes the top-hat type shape. The distribution of water phase is not close to the turbulent pipe flow distribution, the second reason seems to be reasonable in the results. In the figure 12 (b), the distribution shape becomes close to the gaussian distribution and the all phases have almost the same shape. In the edge of the jet, the order of the velocity magnitude is particle, water and single phases. The distribution of the particle velocity becomes flat shape compared with another phases. Adding the particles in the injection jet causes the increase in the water phase velocity.

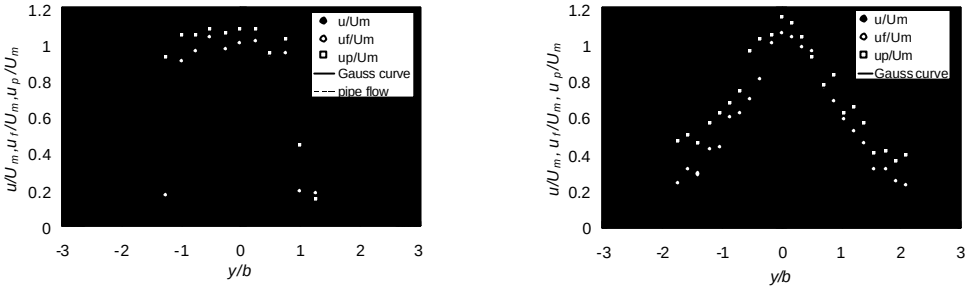

(a) x = 0mm *(b) x = 50mm*

Fig. 12 Distributions of mean axial velocity in dense condition.

Figure 13(a) and (b) shows the fluctuation velocity for x = 0 and 50 mm, respectively. In the figure 13 (a), the fluctuation velocity of the single phase flow is similar as LDA data, and the value is small around the axis and the maximum velocity appears at y/b = 1. However, another phases have quite different shapes compared with single phase flow. The maximum value of particle rms is observed near the center line. The water phase has flat shape in the measuring region. From this result, it seems that the momentum of the particle is large enough to affect the water enhancing the turbulence motion. In the figure 13(b), little larger value can be observed compared with that measured by LDA shown in Fig. 7. It will be caused by the miss optimization of the PDA setting depending on noisy signals. The particle have large values in all the measuring positions. In the edge of the jet, the particle rms is scattered due to poor data number to calculate the rms value. The particles keep large value and the water has also larger value than the single phase flow velocity.

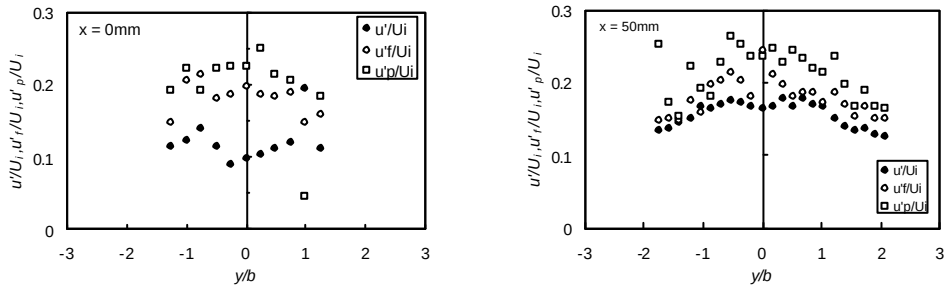

(a) x = 0mm *(b) x = 50mm*

Fig. 13 Fluctuation velocities for dense condition.

In the paper described by Gore and Crowe (1989), the turbulence modification is affected by the ratio between particle diameter and turbulent length scale. In this study, the ratio, which calculated with their method, is the same in the whole region. The turbulence changing rates are dependent on the positions. It seems that all of the results of Figs. 12 and 13 are related with the local mass flux. The local mass flux is estimated in all of the measuring position by using the probe area, particle velocity and particle density. The relationship between the local mass flux and change rate of the turbulence of the water phase is illustrated in Fig. 14. The positive correlation can be observed. The local mass flux is clearly influenced in the turbulence motion.

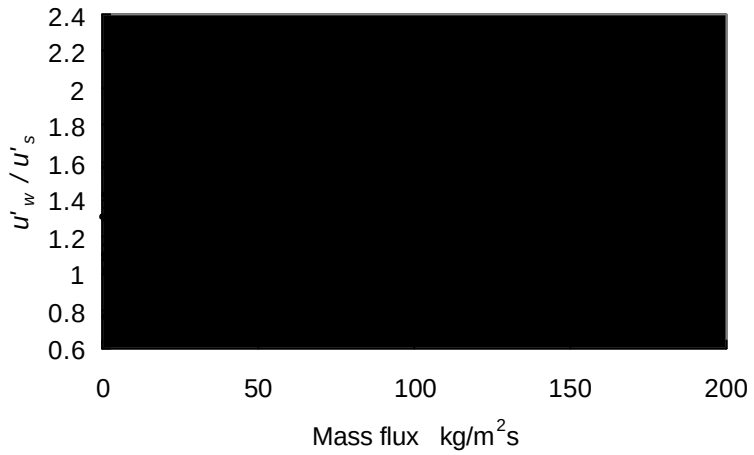

Fig. 14 Correlation between local mass flux and change in turbulence intensity.

3.3 Possibility of PIV measurement

Recently, Particle Image Velocimetry (PIV) is widely applied in the flow velocity measurements. It can measure instantaneous and two-dimensional velocity field. However, when it is applied in the two-phase flow, the problem is how to know or discriminate the particle diameter. Currently, several researchers are working on this problem, i.e. using two CCD camera systems or measurement of laser fluorescence intensity. In this section, small test was carried out to discriminate the particle diameter. All the experimental set up is the same as the above experiment, but the initial velocity is set as 0.7m/s. Figure 15 shows the comparison between results obtained from PIV and PDA. Both experiments are performed under the same condition. The PDA data are divided into particle and water velocities. The PIV results of mean velocity was calculated from average of 70 instantaneous data. The result has similar distribution of the water phase velocity. In the measurements, concentration of seeding particles is much larger than that of glass particles. In the processing of the PIV data, both of the particle and the seeding images are including. When calculating the correlation function, seeding image can get stronger correlation because the number of seeding particles is quite larger than the glass particle. In addition, the PIV data are obtained as averaged value, whereas the grass particle velocity can hardly estimate from the average value. These two reasons cause the PIV data close to the water phase results by PDA.

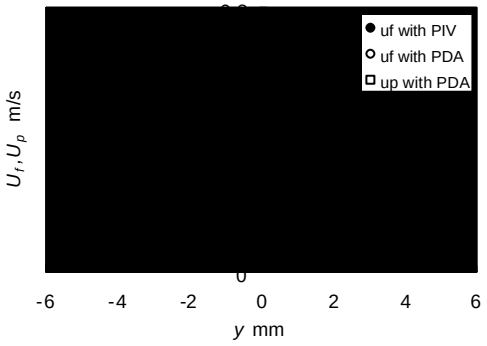

Figure 15 Comparison between both results of PIV and PDA.

The second test was carried out by using the stroboscope light instead of YAG laser. Since it was too difficult to get good picture, the initial jet velocity was set as 0.184 m/s. The result overlapping the original picture is shown in figure 16. For comparison of the both results, YAG laser result is also shown in figure 16. In the results by stroboscope, no vectors can observe in the surrounding water because the scattering light from the seeding particles in the surrounding water is too weak to get good pictures. On the other hand, the results by using the YAG laser can get vectors in the whole measurements region. It could be concluded that stroboscope result has the possibility to get the particle velocity. However, the velocity range has to be small because illuminating time is not controllable and it is too long for the stroboscope to get the particles with large velocity. From the results of the figures 15 and 16, it seems that the possibility of discriminating measurements of the both phase in two-phase flow.

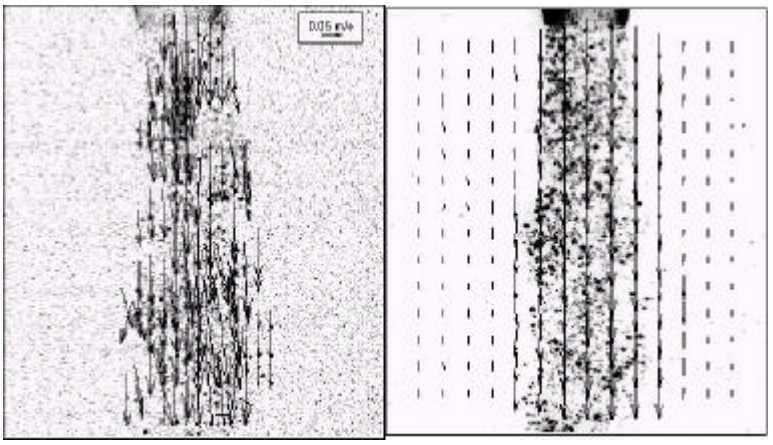

(a) stroboscope light *(b) YAG laser*

Figure 16 Results of PIV measurement by using two-light source.

4. SUMMARY

To study the dominant parameter of the particle dispersion and turbulent modification in solid-water two-phase jet flow, two pipe conditions and two particle loading conditions have been tested in the paper. LDA and PDA are applied to measure the particle motion and turbulence modification. In the PDA measurements, raw data are divided into particle and water phase velocities by using the size information. The possibility of PIV measurement for the two-phase flow was also discussed. The concluding remarks are followings:

The relative velocities in both streamwise and lateral direction is related with Stokes number based on the velocity gradient and particle relaxation time. The particle cannot follow the mean water motion due to the large Stokes number. After the particle can get large Saffman's lift force.

By means of PDA, particle and water velocities can be estimated independently. When particle loading is large, water mean and fluctuation velocities are changed from single phase flow. The local mass flux can help understanding the turbulent modification.

PIV system with the strong light source as YAG laser can provide seeding data in the two-phase flow. The particle velocity vector can be measured by using a stroboscope as a weak light source.

Acknowledgement
The present works were supported by Grant-in-Aid for Encouragement of Young Scientists No. 12750128 by Japan Society for the Promotion of Science in 2000.

REFERENCES

Calabrese, R. V. and Middleman, S. (1976). "The Dispersion of Discrete Particles in a Turbulent Fluid Field", AIChE Journal, 34-6, 946-954.

Chein and Chung (1987)."Effects of Vortex Pairing on Particle Dispersion in Turbulent Shear Flows", Int. J. Multiphase Flow, 13-6, 785-802.

Gore, R. A. and Crowe, C. T. (1989). "Effect of Particle Size on Modulating Turbulent Intensity", Int. J. Multiphase Flow, 15-2, 279-285.

Hardalupas, Y., Taylor, A. M. K. P. and Whitelaw, J. H. (1989). "Velocity and Particle-Flux Characteristics of Turbulent Particle-laden Jets", Proc. R. Soc. Lond. A, 426, 31-78.

Hishida, K., Ando, A. and Maeda, M. (1992). "Experiments on Particle Dispersion in a Turbulent Mixing Layer", Int. J. Multiphase Flow, 18-2, 181-194.

Hishida, K., Nakano, H., Fujishiro, T and Maeda, M (1989). "Turbulence Characteristics of Liquid-Solids Two-Phase Circular Confined Jet (in Japanese)", Transactions of JSME, Series B, 55-511, 648-654.

Ishima, T, Hishida, K. and Maeda, M(1993). "Effect of Particle Residence Time on Particle Dispersion in a Plane Mixing Layer", Transactions of the ASME, Journal of Fluids Engineering, 115-4, 751-759.

Ishima, T., Hishida, K. and Maeda, M. (1994). “Particle Dispersion in Grid Turbulence”, Transactions of JSME, Series B, 60-575, 2391-2396.

Parthasarathy, R. N. and Feath, G. M.(1987). “ Structure of Particle-Laden Turbulent Water Jets in Still Water”, Int. J. Multiphase Flow, 13, 699-716.

Schlichting, T. (1955). “Boundary-Layer Theory”, McGRAW-HILL

Snyder, W.H. and Lumley, J.L. (1971). “Some measurements of particle velocity autocorrelation functions in a turbulent flow”, J. Fluid Mech., 48,part 1, 40-71.

Taylor, G.I. (1921). “Diffusion by Continuous Movements”, Proc.R.Soc.Lond. 20, 196-212.

Wells, M.R. and Stock, D.E. (1983).“The effects of crossing trajectories on the dispersion of particles in a turbulent flow”, J. Fluid Mech., 136, 31-62.